Exploring zero-point energies and hydrogen bond geometries along proton transfer pathways by low-temperature NMR

Sergei N. Smirnov, Hans Benedict, Nikolai S. Golubev, Gleb S. Denisov, Maurice M. Kreevoy, Richard L. Schowen, and Hans-Heinrich Limbach

Abstract: We have followed by NMR the zero-point energy changes of the hydrogen bond proton in 1:1 acid–base complexes AHB ≡ {A—H···B ↔ $A^{\delta-}$···H···$B^{\delta+}$ ↔ A^{-}···H—B^{+}} as a function of the proton position between A and B. For this purpose, the isotopic fractionation factors K between the acid–base complexes AHB + Ph_3COD···B ⇆ ADB + Ph_3COH···B, where AH represents a variety of acids and B represents pyridine-^{15}N, were measured around 110 K, using a 2:1 mixture of liquefied $CDClF_2$–CDF_3 as solvent. As under these conditions the slow hydrogen bond exchange regime is reached, the values of K could be obtained directly by integration of appropriate proton NMR signals. Using the valence-bond order concept established previously by crystallography, the fractionation factors and corresponding zero-point energy changes (ΔZPE) are related in a quantitative way to the hydrogen bond geometries, the ^{1}H chemical shift of the hydrogen bond proton, and the pyridine-^{15}N chemical shift. The K values are related in a quasi-linear way to the chemical shifts of the hydrogen bond proton, where the slope depends on whether the proton is closer to oxygen or nitrogen. In the region of the strongly hydrogen-bonded quasi-symmetric complexes, which are characterized by a strong hydrogen bond contraction, the variation of K is very small in spite of substantial proton displacements.

Key words: NMR, isotopic fractionation, hydrogen bonding, acid–base complexes, proton transfer, geometric isotope effects.

Résumé : Faisant appel à la RMN, on a suivi les changements d'énergie du point zéro du proton de la liaison hydrogène de complexes acide–base 1 : 1 AHB ≡ {A—H···B ↔ $A^{\delta-}$···H···$B^{\delta+}$ ↔ A^{-}···H—B^{+}} en fonction de la position du proton entre A et B. À cette fin, opérant à environ 110 K et utilisant un mélange 2 : 1 liquéfié de $CDClF_2$: CDF_3 comme solvant, on a mesuré les facteurs de fractionnement isotopiques, K, entre les complexes acide–base, AHB + Ph_3COD···B ⇆ ADB + Ph_3COH···B, dans laquelle AH représente une variété d'acides et B correspond à pyridine-^{15}N. Dans de telles conditions, on atteint un régime d'échange lent de la liaison hydrogène et il est possible de déduire les valeurs de K directement par intégration des signaux RMN des protons appropriés. Utilisant le concept d'ordre de la liaison de valence mis au point antérieurement par cristallographie, on peut établir une corrélation quantitative entre les facteurs de fractionnement ou les changements correspondants dans les énergies de point zéro (« ΔZPE ») et les géométries de la liaison hydrogène, le déplacement chimique ^{1}H du proton de la liaison hydrogène et le déplacement chimique de la pyridine-^{15}N. On peut établir une corrélation pratiquement linéaire entre les valeurs de K et les déplacements chimiques du proton de la liaison hydrogène; la pente dépend de la distance entre le proton et l'oxygène ou l'azote. Dans la région de forte liaison hydrogène où les complexes sont pratiquement symétriques et qui est caractérisée par une forte contraction de la liaison hydrogène, la variation de K est très faible malgré le fait que les déplacements de proton soient importants.

Mots clés : RMN, fractionnement isotopique, liaison hydrogène, complexes acide–base, transfert de proton, effets isotopiques géométriques.

[Traduit par la Rédaction]

Received January 9, 1999.

This paper is dedicated to Jerry Kresge in recognition of his many achievements in chemistry.

S.N. Smirnov and N.S. Golubev. Institut für Organische Chemie, Freie Universität Berlin, Takustrasse 3, D-14195 Berlin, Germany, and the Institute of Physics, St. Petersburg State University, 198904 St. Petersburg, Russian Federation.
H. Benedict, and H.-H. Limbach.[1] Institut für Organische Chemie, Freie Universität Berlin, Takustrasse 3, D-14195 Berlin, Germany.
G.S. Denisov. Institute of Physics, St. Petersburg State University, 198904 St. Petersburg, Russian Federation.
M.M. Kreevoy. Department of Chemistry, University of Minnesota, Kolthoff & Smith Halls, 207 Pleasant Street, Minneapolis, MN 55455, U.S.A.
R.L. Schowen. Departments of Chemistry and Biochemistry, University of Kansas, Lawrence, KS 66045, U.S.A.

[1]Author to whom correspondence may be addressed. Fax: 49 30 838-5310. e-mail: limbach@chemie.fu-berlin.de

Introduction

It has been known for a long time that H/D isotopic fractionation between different proton donor sites is mainly caused by zero-point energy changes between the sites (1). The measurement of fractionation factors using a variety of methods is, therefore, an established tool of isotopic research (2). On the other hand, fractionation factor theory in combination with transition state theory constitutes the classical theory of kinetic H/D isotope effects of proton transfer reactions (1, 3). However, proton tunneling through the reaction barrier is another source of kinetic isotope effects (4), and it is thus often difficult from an experimental standpoint to decide which effect causes the observed kinetic H/D isotope effects. As proton transfer is an elementary step of many organic and biochemical reactions (5–7) and is interesting from a theoretical standpoint, it would be desirable if one could follow directly the proton transfer pathways and the associated zero-point energy changes. Since this is experimentally very difficult, the study of model hydrogen-bonded systems is of great help where each system models a typical point or region of the reaction coordinate. For example, using a series of hydrogen-bonded anions, Kreevoy and Liang (2*a*) determined fractionation factors as a function of the hydrogen bond geometry using UV spectroscopy. However, using this method it is difficult to follow, at the same time, changes in the hydrogen bond geometries.

Recently some of us (8) have proposed a model series for the pathway of a proton from an acid (AH) to a base (B) that can conveniently be studied by low-temperature liquid state NMR (9) around 110 K using liquefied deuterated gases as solvents. This method allows one to distinguish different hydrogen-bonded species $(AH)_nB_m$ in the slow-exchange regime, in contrast to the usual NMR spectroscopy where only average signals are observed. Thus, the NMR properties of simple neutral 1:1 complexes of the type AHB $\equiv$ {A—H···B $\leftrightarrow$ $A^{\delta-}$···H···$B^{\delta+}$ $\leftrightarrow$ A^-···H—B^+} could be studied, in which the proton was gradually displaced from the acid AH to the acceptor B, $\equiv$ pyridine-^{15}N, by changing the proton-donating power of AH. The optical spectroscopy of such complexes is well known (for references concerning properties of pyridine – carboxylic acid complexes, see ref. 10). During this displacement, characteristic changes of NMR chemical shifts and coupling constants were observed, including H/D isotope effects in the former that were qualitatively related to associated changes of the hydrogen bond geometries (8*d*). Such effects were quantified in other model systems using solid state NMR and theoretical methods (11).

In this paper we extend the low-temperature NMR technique to the measurement of the equilibrium constants K of isotopic fractionation between AHB with respect to a reference XH or XHB. Therefore, the fractionation factors measured here are defined by the equations

$$[1] \qquad \mathrm{AHB} + \mathrm{XDB} \overset{K}{\rightleftarrows} \mathrm{ADB} + \mathrm{XHB}$$

$$[2] \qquad K = \frac{x_{\mathrm{XHB}}\, x_{\mathrm{ADB}}}{x_{\mathrm{XDB}}\, x_{\mathrm{AHB}}} \approx \exp\left(-\Delta\mathrm{ZPE}/RT\right)$$

R is the gas constant, T the temperature, x the mole fractions or concentrations, and ΔZPE the zero-point energy difference given by

$$[3] \qquad \Delta\mathrm{ZPE} = \mathrm{ZPE(XHB)} - \mathrm{ZPE(XDB)} + \mathrm{ZPE(ADB)} - \mathrm{ZPE(AHB)}$$

The idea was that using the low-temperature NMR technique it should be possible to determine K directly by integration of appropriate NMR signals as the slow hydrogen bond and proton exchange regime can be reached. However, as this concept had not yet been realized, the setup of the technique was not trivial. Especially difficult was the choice of the reference proton donor XH. We tried out different acids and found that acetic acid (AcOH) is a good choice from the standpoint of the experimental technique. In a later stage of this study we found that triphenylmethanol is a reference that is more closely related than AcOH to the usual standard, water, because the fractionation factor of Ph_3COH in acetonitrile with respect to water is unity; moreover, this alcohol shows little evidence of self-association (2*a*). Thus we succeeded in measuring K for a number of AHB complexes with respect to the 1:1 complex of Ph_3COH with pyridine.

In the following, after a short experimental section, the results are presented and discussed qualitatively in terms of an appropriate hydrogen bond geometry correlation analysis.

Experimental section

All NMR experiments reported in this paper were performed on a Bruker NMR AMX 500 instrument operating at 500.13 MHz for ^{1}H. The details of these experiments have been reported previously (8*d*). Pyridine-^{15}N (95% enriched) was purchased from Chemotrade, Leipzig, Germany. CH_3COOD was purchased from Aldrich; the other acids were deuterated using either D_2O or CH_3OD. The deuterated freon solvent mixture $CDClF_2$:CDF_3 (2:1) freezes below 90 K. It was synthesized, as described previously (9), at 100°C and elevated pressures (between 30 and 60 bar (1 bar = 100 kPa)) from $CDCl_3$ via fluorination with $SbF_3/SbCl_5$. The solvent was handled on a vacuum line and stored over basic alumina in order to remove traces of acids and water. The vacuum line also served to prepare the samples using well-established techniques (4*d*). No special effort was made to remove water from the solutes employed as water traces precipitate in freons at low temperature. Each sample consisted of comparable amounts of the partially deuterated acid for which the fractionation factor was to be determined, of acetic acid-*d*, of a small excess of pyridine-^{15}N with respect to both acids, and of about 0.5 mL of the solvent. The concentrations of the solutes refer to room temperature and were determined prior to the sample preparation either by weighing, in the case of solids, or by volumetric measurements on the vacuum line in the case of liquid components as described previously (4*d*). The fractionation factors K for a given complex AHB referring to Ph_3COH···B were determined from the low-temperature ^{1}H NMR spectra using the equation

$$[4] \qquad K' = K/K'(\mathrm{Ph_3COH}) = \frac{I_{\mathrm{CH}}\left(I_{\mathrm{CH}} - I_{\mathrm{AHB}}\right)}{I_{\mathrm{AHB}}\left(I_{\mathrm{CH3}}/3 - I_{\mathrm{AcHB}}\right)}$$

which can easily be derived from eq. [2]. $K'(Ph_3COH)$ is the H/D-fractionation factor for $Ph_3COH\cdots B$ with respect to the acetic acid – pyridine complex, I_{CH3} the intensity of the methyl group signal of acetic acid, I_{CH} the sum of the intensities of the CH proton signals for AHB and ADB, I_{AcHB} the intensity of the H-bonded proton signal for the 1:1 acetic acid – pyridine complex, I_{AHB} the intensity of the H-bonded proton signal for AHB. The relative solute mole fractions determined by signal integration of the low-temperature spectra were slightly different from those calculated from the total concentrations determined as described above. However, as the absolute concentrations do not enter eq. [4] and as small variations of the concentrations do not affect the intrinsic chemical shifts of the acid–base complexes, no attempt was made to determine the correct concentrations, which are also temperature dependent because of the temperature dependence of the solvent density.

Results

Typical low-temperature ^1H NMR spectra of equilibrated solutions containing a partially deuterated acid, AL (L = H, D), a comparable amount of CH_3COOL (AcOL), and of pyridine-^{15}N in small molar excess over both acids combined, dissolved in a 2:1 mixture of liquefied $CDClF_2$:CDF_3, are shown in Figs. 1*a* and 1*b*. Under these conditions the acids form only 1:1 complexes with pyridine, B (8*d*), and the complexation of the acids is essentially complete. Each solution gives rise to two low-field signals in its ^1H NMR spectrum: one for AHB and one for the complex with acetic acid, AcOHB. As the slow hydrogen bond regime is reached, the chemical shifts observed are the intrinsic values referring to the 1:1 complexes and are not affected by small concentration variations. As discussed previously (8*e*, 8*h*), the intrinsic chemical shifts depend on temperature because of a temperature-dependent solvent ordering causing changes in the hydrogen bond geometries. The mobile protons in the two sites exchange slowly on the timescale of seconds, as shown by a differential NOE experiment depicted in Fig. 1*c*, where the acetic acid peak at 17.65 ppm was irradiated and a positive formic acid – pyridine peak at 21 ppm indicated a slow magnetization transfer by chemical exchange between the two mobile proton sites. However, the exchange is complete on the timescale of many minutes, as shown by the invariance with time of the relative integrated areas. The fractionation factors are easily obtained by signal integration using eq. [4]. The results of the measurements are assembled in Table 1 and Fig. 2, which contain also the ^1H and ^{15}N chemical shifts reported previously (8d); the shifts of triphenylmethanol, methylaniline, and 4-*tert*-butylphenol were determined in this study.

Discussion

We have measured the H/D fractionation factors K of 1:1 hydrogen-bonded complexes of various proton donors with pyridine by low-temperature NMR spectroscopy in the slow hydrogen bond exchange regime, using Ph_3COH with an excess of pyridine as a reference. We note from Table 1 that the OH chemical shift of this donor is around 10 ppm at 112 K, as compared to the neat compound exhibiting an OH

Fig. 1. Partial 500 MHz ^1H NMR spectra of solutions of pyridine-^{15}N (B)/acetic acid (AcOH)/variable acid AH in a 2:1 mixture of $CDClF_2$:CDF_3 at non-zero deuterium fractions D in the mobile proton sites. (*a*) AH ≡ dichloroacetic acid, uncorrected concentrations at room temperature C_B = 0.058, $C_{AH} + C_{AD}$ = 0.011 mol L^{-1}, $C_{AcOH} + C_{AcOD}$ = 0.038 mol L^{-1}, T = 107 K. (*b*) AH ≡ formic acid, uncorrected concentrations at room temperature C_B = 0.033 mol L^{-1}, $C_{AH} + C_{AD}$ = 0.019 mol L^{-1}, $C_{AcOH} + C_{AcOD}$ = 0.011 mol L^{-1}, T = 109 K. (*c*) NOE difference spectrum of the sample in Fig. 1*b*, where the hydrogen-bonded proton of acetic acid at 17.65 ppm was irradiated.

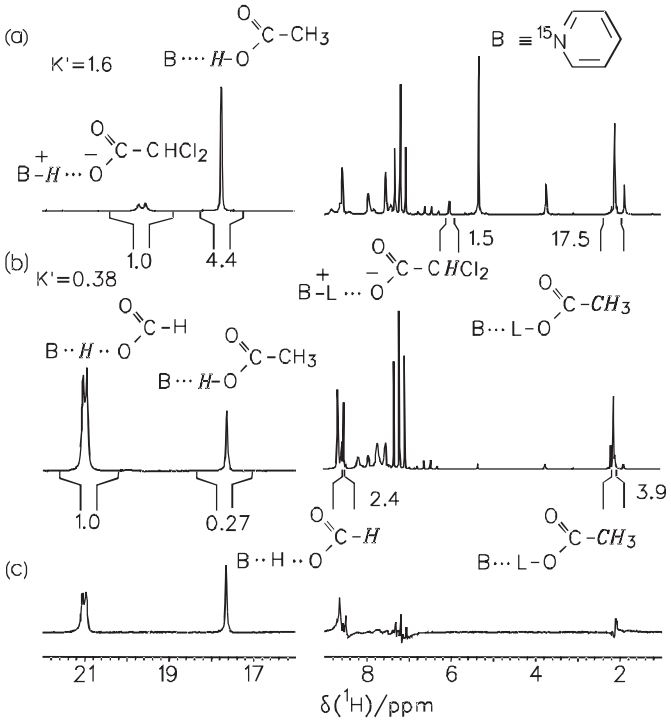

chemical shift of about 5 ppm at room temperature. The ^{15}N chemical shift of pyridine in the presence of Ph_3COH is slightly shifted upfield, indicating that Ph_3COH forms a weak 1:1 hydrogen bond with pyridine. Therefore, we conclude that the complex $Ph_3COH\cdots B$ is the true reference for the fractionation factors K, as indicated by eqs. [1] and [2]. As the fractionation factor between Ph_3COH and water in acetonitrile is close to unity (2*a*), the fractionation factors reported here are good estimates for those referring to water.

To facilitate the discussion of our results we first review the concept of the valence bond order for the estimation of hydrogen bond geometries. This concept goes back to the valence bond – length relationship developed by Pauling and Brown (14). It states that one can associate with any bond between two atoms i and j an empirical valence bond order p_{ij}, which decays exponentially with the bond distance r_{ij}, i.e.,

$$[5] \qquad p_{ij} = \exp\{-(r_{ij} - r_{ij}^0)/b_{ij}\}$$

where b_{ij} is a decay parameter and r_{ij}^0 the distance where p_{ij} = 1. A hydrogen-bonded system, e.g., an O—H···N hydrogen bond (Scheme 1), is then characterized by two bond orders p_{OH} and p_{HN} involving the hydrogen-bonded proton. As the total valency of hydrogen is unity,

Table 1. Fractionation factors and chemical shifts of 1:1 hydrogen-bonded complexes of acids AH with pyridine-^{15}N (B) dissolved in a 2:1 mixture of $CDClF_2$:CDF_3.[a]

AH	pK_a (ref.)	C_{AL}	C_{AcOL}	C_B	T/K	$\delta(^1H)$	$\delta(^{15}N)$	K' [c]	K
Triphenylmethanol	12.9 (13*a*)	0.025	0.018	0.045	112	9.95	–7.0[b]	2.8	1.0
4-*tert*-Butylphenol	10.23 (13*b*)	0.013	0.014	0.032	108	13.264	–16.0	1.94	0.69
Acetic acid	4.75 (13*c*)	0.037	0.037	0.07	111	17.65	–27.9	1.00	0.36
o-Toluic acid	3.91 (13*c*)	0.012	0.011	0.027	107	19.202	–33.7	0.66	0.24
3-Br-propionic acid	3.89 (13*d*)	0.014	0.014	0.030	108	19.949	–41.6	0.52	0.19
Formic acid	3.75 (13*c*)	0.019	0.011	0.033	109	21.009	–59.0	0.38	0.14
2-Furoic acid	3.17 (13*e*)	0.020	0.036	0.064	107	21.467	–70.8	0.52	0.19
Chloroacetic acid	2.85 (13*c*)	0.017	0.020	0.048	107	20.824	–79.5	0.76	0.27
Dichloroacetic acid	1.48 (13*c*)	0.011	0.038	0.058	107	19.637	–89.4	1.6	0.57
N-Methylaniline	29.5 (13*f*)	0.017	0.015	0.037	111	3.95	–0.01	2.8	1.0

[a] $C_{AL} = C_{AH} + C_{AD}$ and C_B total concentrations (uncorrected, see experimental section) of the acid AH and of pyridine–^{15}N in mol L^{-1} determined at room temperature. AcOH ≡ acetic acid. The chemical shifts $\delta(^1H)$ and $\delta(^{15}N)$ are taken from ref. 8*d*, with the exception of those of *N*-methylaniline, triphenylmethanol, and 4-*tert*-butylphenol (this study).

[b] 1:1 Ph_3COH:pyridine-^{15}N complex in CD_2Cl_2, 170 K. The $\delta(^{15}N)$ are referenced to internal or free pyridine, where $\delta(CH_3NO_2) = \delta(C_5H_5N) - 69.2$ ppm, and $\delta(NH_4Cl) = \delta(CH_3NO_2) - 338$ ppm (12). The pK_a values were taken from ref. 13 and refer to aqueous solutions at 298 K.

[c] *K'*: fractionation factor referred to the 1:1 complex of acetic acid with pyridine and *K:* fractionation factor referred to the triphenylmethanol–pyridine complex. The errors in the fractionation factors could not be determined precisely, but are estimated in the region of 10–20%.

Fig. 2. (*a*) Hydrogen bond correlation curve for (dotted line) 1:1 hydrogen-bonded acid–base complexes according to refs. 8*d* and 11*b*. $q_2 = r_1 + r_2$ represents the heavy atom distance for the case of a linear hydrogen bridge, $q_1 = 1/2(r_1 - r_2)$ the proton transfer coordinate. The filled circles represent the geometries of the corresponding chemical shift data points in Fig. 2*b*. (*b*) Low-temperature NMR chemical shifts of the hydrogen bond proton in 1:1 complexes between acids and pyridine-^{15}N dissolved in a 2:1 CDF_2Cl:CDF_3 mixture as a function of the ^{15}N chemical shifts. Reference: solid NH_4Cl, where $\delta(NH_4Cl) = \delta(CH_3NO_2) - 353$ ppm (12). In the initial measurement (8*d*) internal pyridine-^{15}N was used as a reference, where $\delta(CH_3NO_2) = \delta(C_5H_5N) - 69.2$ ppm. (*c*) Corresponding fractionation factors *K* (circles) and zero-point energy differences ΔZPE (squares) as a function of the ^{15}N chemical shifts. (*d*) Fractionation factors *K* as a function of the proton chemical shifts. The dotted lines in (*b*) to (*c*) were calculated as described in the text. The broken limits correspond to infinite values of q_1 and q_2.

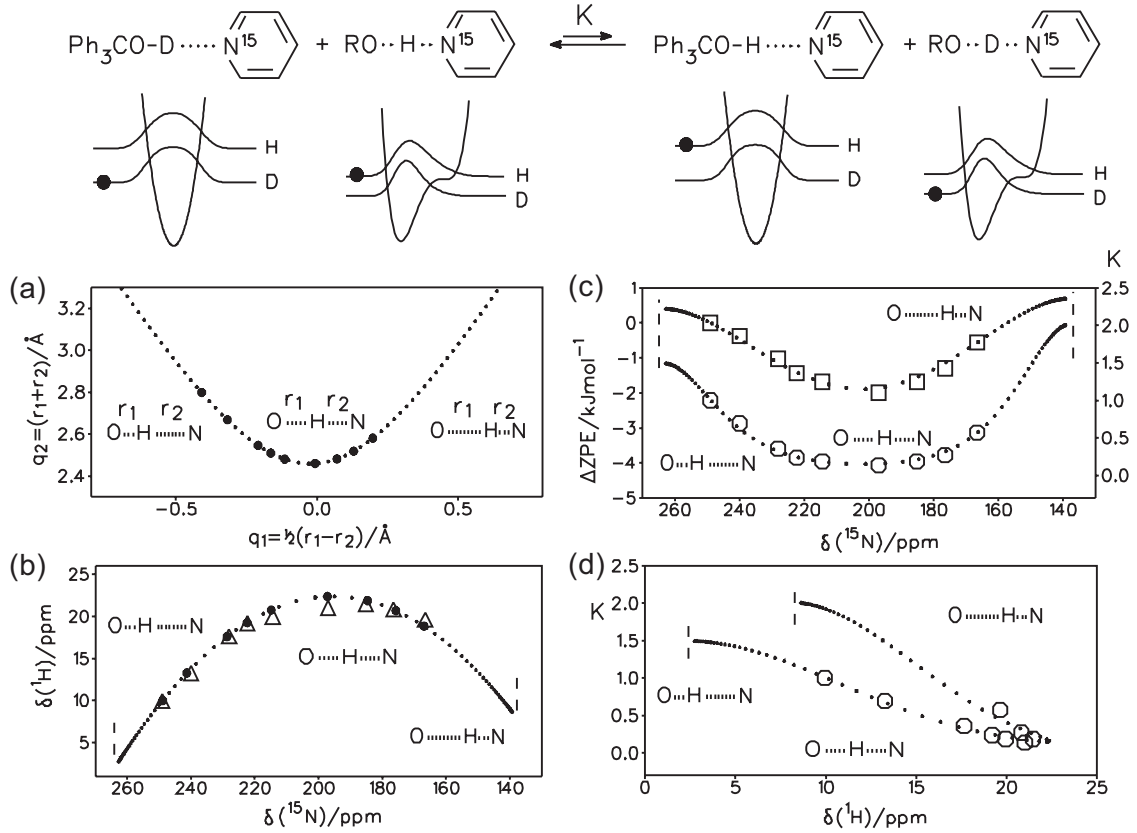

Scheme 1.

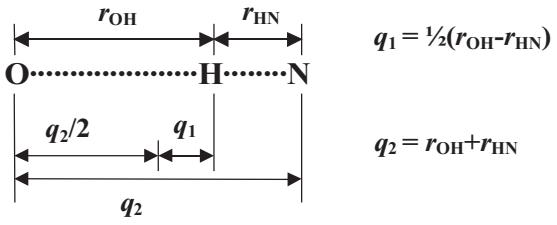

$$[6] \quad p_{OH} + p_{HN} = 1 = \exp\{-(r_{OH} - r_{OH}^0)/b_{OH}\} + \exp\{-(r_{HN} - r_{HN}^0)/b_{HN}\}$$

it follows that the two bond distances r_{OH} and r_{HN} cannot be varied independently. Naturally, this prediction implies at the same time a correlation between q_1 and q_2, defined in Scheme 1. For a linear hydrogen bond, q_1 corresponds to the distance of the proton or deuteron from the center of the hydrogen bond, i.e., it represents the proton transfer coordinate, and q_2 is equal to the A···B distance (11*b*) The dependence of q_1 as a function of q_2 can be obtained easily from the definition in Scheme 1 and eq. [6].

Hydrogen bond correlations have been established by crystallography (15) by comparing the neutron crystal structures of a large number of systems exhibiting hydrogen bonds of weak and medium strength. The curves depend only on the type of donor and acceptor atoms, i.e., OHO, OHN, and NHN bonds exhibit different parameters in eq. [6]. The NHN bond correlation has been verified by some of us (11*b*) using solid state NMR and theoretical calculations. In conclusion, the valence bond order model does not distinguish qualitatively but only quantitatively between the covalent bond and the hydrogen bond.

For the case of O—H···N bonds, Steiner (15*d*) has proposed the parameter set $r_{OH}^0 = 0.942$ Å, $r_{HN}^0 = 0.992$ Å, $b_{OH} = 0.371$ Å, $b_{HN} = 0.385$ Å. Using these values, we have calculated the correlation curve $q_1 = f(q_2)$ depicted in Fig. 2*a*. The curve indicates that when the proton is transferred from O to N the O···N distance first shortens, then reaches a minimum in the quasi-symmetric complex, and finally widens again as the zwitterionic complex is approached.

Figure 3 shows in more detail, in a qualitative way, what exactly may happen during the transfer process. Two limiting cases are represented. In Fig. 3*a* the proton exhibits a medium barrier for proton transfer at the quasi-symmetric midpoint whereas such a barrier is absent in Fig. 3*b*. In the case of Fig. 3*a* the solute–solvent interaction may easily break the symmetry of the potential, leading to a proton transfer equilibrium between two strongly hydrogen-bonded states, characterized by a common value of q_2 but different values $-q_1$ and $+q_1$, i.e., q_2 will not reach the minimum value. Generally, deuteration leads to a primary geometric H/D isotope effect on q_1 and to a secondary effect on q_2 (8*d*, 11*b*). The latter effect was found by Ubbelohde and Gallagher (16) and is also called the Ubbelohde Effect. If there is a barrier to the proton motion, the secondary isotope effect is always directed in such a way that the A···B distance increases after deuteration. On the other hand, the primary geometric isotope effect implies a larger distance to the hydrogen bond center for the deuteron than for the proton (11*b*). The primary and secondary geometric isotope effects are similar in the no-barrier case of Fig. 3*b*, as well as around the quasi-symmetric midpoint where the A···B distance can contract slightly after deuteration because of the smaller width of the deuteron wave function in the vibrational ground state (12*b*).

Fig. 3. One-dimensional hydron (L = H, D) potentials and geometric changes during the transfer of a hydron from A to B characterized by the reaction coordinate $q_1 = 1/2(r_1 - r_2)$. The squares of the wave functions of the vibrational ground states for H and D, i.e., the proton and deuteron distribution functions, are included. (*a*) Case involving a medium proton transfer barrier at the quasi-symmetric midpoint. (*b*) Case involving a very small or no barrier at the quasi-symmetric midpoint. For further explanation see text. Adapted from ref. 8*d*.

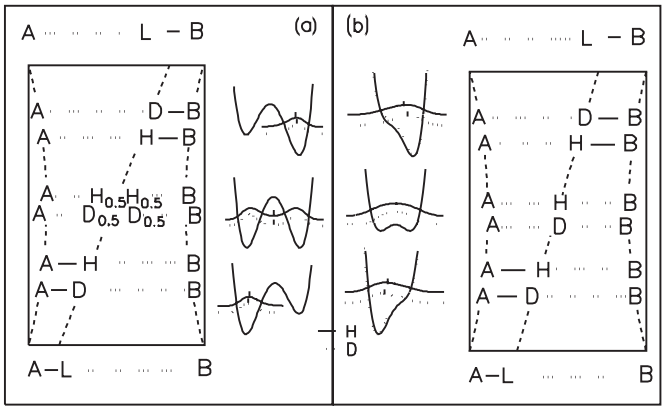

In the latter paper, the hydrogen bond correlation concept was extended to other hydrogen bond properties. Thus, empirical equations were presented relating the geometric H/D isotope effects, zero-point energy changes, ^{1}H and ^{15}N chemical shifts to derivatives, or combinations of various derivatives of the correlation of eq. [7]. However, the equations presented referred only to the symmetric case of NHN hydrogen bonds. Here, we had to treat the unsymmetrical NHO case. During this work we found that it is possible to expand all correlations directly in terms of the valence bond orders, which constitutes a considerable simplification. For example, we observe that the ^{15}N chemical shifts can be expressed by

$$[7] \quad \delta_N = \delta_N^\infty - (\delta_N^\infty - \delta_{HN}^0)p_{HN}$$
$$\delta_N^\infty = 264 \text{ ppm and } \delta_{HN}^0 = 138 \text{ ppm}$$

where the parameters δ_N^∞ and δ_{HN}^0 are the values of free pyridine and of the isolated pyridinium where $r = r_{HN}^0 = 0.992$ Å. For the ^{1}H chemical shifts we find empirically that

$$[8] \quad \delta(^1H) = 4\Delta_H p_{OH} p_{HN} + \delta_{OH}^0 p_{OH} + \delta_{HN}^0 p_{HN}$$
$$\Delta_H = 17.25 \text{ ppm}, \delta_{OH}^0 = 2 \text{ ppm, and } \delta_{HN}^0 = 8 \text{ ppm}$$

Δ_H is the excess chemical shift of the quasisymmetric complex and δ_{OH}^0 and δ_{HN}^0 the limiting chemical shifts corresponding to the distances $r_{OH}^0 = 0.942$ Å and $r_{HN}^0 = 0.992$ Å. It is clear that, because of eq.[6], $\delta(^1H)$ must be correlated with $\delta(^{15}N)$, which is indeed the case as depicted by the dotted line in Fig. 2*b*. This curve was generated by calculating

$\delta(^1H)$ and $\delta(^{15}N)$ from an arbitrary grid of q_1 values. The parameters in eqs. [7] and [8] were adjusted by "eye-fitting" the calculated dotted line in Fig. 2*b* to the experimental values taken from ref. 8*d*. The agreement is very satisfactory. We note that the $\delta(^1H)$ vs. $\delta(^{15}N)$ correlation curve exhibits a principal difference from the q_1 vs. q_2 curve of Fig. 2*a* because the distance between the separate residues AH and B can be varied in an infinite number of ways during which their chemical shifts remain constant. Therefore, the dotted correlation line in Fig. 2*b* ends at the left and the right sides as illustrated by the vertical bars. Finally, we note that the experimental chemical shift data of Fig. 2*b* can be easily converted into distances as indicated by the filled circles of Figs. 2*a* and 2*b*.

Let us now discuss the graph of Fig. 2*c* where we have plotted the fractionation factors *K* of Table 1 (lower graph) and the corresponding values of ΔZPE (upper graph), as defined in eq. [2], as a function of $\delta(^{15}N)$. Previously (11*b*), we had noted for the NHN case that ΔZPE is proportional to the square of the second derivative of q_2. Here, we find a simpler equation, valid also in the unsymmetric NHO case, i.e.,

$$[9] \quad \Delta ZPE = \Delta ZPE^{o}(4p_{OH}p_{HN})^2 + \Delta ZPE(OH)^0 p_{OH} + \Delta ZPE(HN)^0 p_{NH}$$

$$\Delta ZPE^0 = -2.44 \text{ kJ mol}^{-1},$$

$$\Delta ZPE(OH)^0 = +0.4 \text{ kJ mol}^{-1},$$

$$\Delta ZPE(HN)^0 = +0.7 \text{ kJ mol}^{-1}$$

Here, $\Delta ZPE(OH)^0$ and $\Delta ZPE(HN)^0$ are the zero-point energy differences of the limiting states where $r_{OH}{}^0 = 0.942$ Å and $r_{HN}{}^0 = 0.992$ Å with respect to our reference complex $Ph_3COH\cdots B$. ΔZPE^0 determines the total drop of the zero-point energy at the quasi-symmetric midpoint with respect to the limiting states. Again, the parameters of eq. [9] were adapted by eye-fitting the calculated values of ΔZPE as a function of $\delta(^{15}N)$ to the experimental values reported in Table 1, leading to the upper dotted line in Fig. 2*c*. We find that the reference $Ph_3COH\cdots B$ exhibits a small drop in the zero-point energy of 0.4 kJ mol^{-1} with respect to the hypothetical free proton donor ROH. Moreover, the experimental value of ΔZPE^0 is smaller than the value of –4 kJ mol^{-1} calculated previously (11*b*) for the anion $[C{\equiv}N\cdots H\cdots N{\equiv}C]^-$. In this case the situation corresponds to Fig. 3*b*. The lower graph in Fig. 2*c* is the straightforward extension of the upper graph, considering eq. [2] and the average temperature of about 120 K at which the experiments were performed. The fractionation factor of 0.2 at 110 K would correspond to about 0.5 at 298 K. The experimental finding of a reduced isotopic fractionation as compared to $[C{\equiv}N\cdots H\cdots N{\equiv}C]^-$ is then consistent with the situation depicted in Fig. 3*a*, where solute–solvent interactions, however, destabilize the quasi-symmetric configurations, hence leading to a smaller extent of the maximum zero-point energy losses. On the other hand, it could also be that the real drop of the hydrogenic stretching frequency in $[C{\equiv}N\cdots H\cdots N{\equiv}C]^-$ is smaller than was calculated and is partly compensated for by an increased in-plane and (or) out-of-plane bending vibrational frequency that was not included in the calculations of ref. 11*b*.

In any case, Fig. 2*c* indicates a quite flat central region in which the fractionation factors *K* do not exhibit major changes although the proton is displaced by about 0.3–0.4 Å in this region, as estimated from Fig. 2*a*. If we take the series of complexes presented in this paper as models of transition states of proton transfer and the fractionation factors as classical kinetic H/D isotope effects, this result would mean that proton motions in strong hydrogen bonds may fail to appear to be contributing substantially to the overall observed kinetic isotope effect, as discussed recently by some of us (5*m*).

Finally, we have plotted in Fig. 2*d* the experimental fractionation factors as a function of the ^1H chemical shifts. The calculated dotted line was here obtained from eqs. [8] and [9]. We find that, in addition to some curvature, *K* is an almost linear function of $\delta(^1H)$, exhibiting, however, a different slope on both sides of the quasi-symmetric complex characterized by the lowest value of *K* and the largest value of $\delta(^1H)$. The slopes are different depending on whether the proton is closer to oxygen or nitrogen. Thus, $\delta(^1H)$ is a qualitative measure, not only of the A···B distance but also of the fractionation factor.

Conclusions

In conclusion, the development of low-temperature NMR makes it possible not only to obtain information on the geometries and on geometric H/D isotope effects but also of isotopic H/D fractionation in a series of intermolecular low-barrier hydrogen-bonded 1:1 acid–base complexes because the slow hydrogen bond exchange regime is reached. Thus, interesting information can be obtained about zero-point energy changes along the reaction pathways of proton transfer. A task of the future will be to study experimentally the hydrogen bond vibrations in this series and to provide a full theoretical treatment of the experimental findings.

Acknowledgements

We thank the Stiftung Volkswagenwerk, Hannover, the Deutsche Forschungsgemeinschaft, Bonn – Bad Godesberg, the Fonds der Chemischen Industrie, Frankfurt, and the Russian Foundation for Fundamental Research for financial support. R.L.S. thanks the Alexander von Humboldt Foundation, Bonn – Bad Godesberg, for a Humboldt award.

References

1. (*a*) J. Bigeleisen and M. Wolfsberg. Adv. Chem. Phys. **1**, 15 (1958); (*b*) R.A. More O'Ferrall. *In* Proton transfer reactions. *Edited by* E.F. Caldin and V. Gold. Chapman and Hall, London. 1975. Chap. 8. pp. 201–262.
2. (*a*) M.M. Kreevoy and T.M. Liang. J. Am. Chem. Soc. **102**, 361 (1980); (*b*) R. Bone and R. Wolfenden. J. Am. Chem. Soc. **107**, 4772 (1985); (*c*) Y. Chiang, A.J. Kresge, T.K. Chang, M.F. Powell, and J.A. Wells. J. Chem. Soc. Chem. Commun. 1587 (1995); (*d*) S.N. Loh and J.L. Markley. Biochemistry, **33**, 1029 (1994); (*e*) C.H. Arrowsmith, H.X. Guo, and A.J. Kresge. J. Am. Chem. Soc. **116**, 8890 (1994); (*f*) V.J. Shiner, Jr. and T.E. Neumann. Z. Naturforsch. A: Phys. Sci. **44**, 337 (1989);

(*g*) R.M. Jarret and M. Saunders. J. Am. Chem. Soc. **107**, 2648 (1985); (*h*) L. Baltzer and N.A. Bergman. J. Chem. Soc. Perkin Trans. 2, 313 (1982); (*i*) V. Gold and S. Grist. J. Chem. Soc. B: 1665 (1971); (*j*) V. Gold and C. Tomlinson. J. Chem. Soc. B, 1707 (1971); (*k*) J.M.A. Al-Rawi, J.P. Bloxsidge, J.A. Elvidge, J.R. Jones, and R.A. More O'Ferrall. J. Chem. Soc. Perkin Trans. 2, 1593 (1979); (*l*) P. Salomaa. Acta Chem. Scand. **23**, 2095 (1969); (*n*) W.P. Jencks and K. Salvesen. J. Am. Chem. Soc. **93**, 4433 (1971).

3. (*a*) L. Melander. Isotope effects on reaction rates. Ronald, New York. 1960. p. 24; (*b*) F.H. Westheimer. Chem. Rev. **61**, 265 (1961).
4. (*a*) R.P. Bell. The tunnel effect. Chapman and Hall, London. 1980; (b) E. Caldin and V. Gold. Proton transfer. Chapman and Hall, London. 1975; (*c*) L. Melander and W.H. Saunders. Reaction rates of isotopic molecules. John Wiley & Sons, New York, Toronto. 1980; (*d*) H.H. Limbach. NMR, **26**, 66 (1991); (*e*) J. Braun, R. Schwesinger, P.G. Williams, H. Morimoto, D.E. Wemmer, and H.H. Limbach. J. Am. Chem. Soc. **118**, 11101 (1996); (*f*) Ch. Hoelger, B. Wehrle, H. Benedict, and H.H. Limbach. J. Phys. Chem. **98**, 843 (1994).
5. (*a*) C.G. Swain, D.A. Kuhn, and R.L. Schowen. J. Am. Chem. Soc. **87**, 1553 (1965); (*b*) R. Eliason and M.M. Kreevoy. J. Am. Chem. Soc. **100**, 7037 (1978); (*c*) W.W. Cleland and M.M. Kreevoy. Science, **264**, 1887 (1994); (*d*) C.L. Perrin. Science, **266**, 1665 (1994); (*e*) D.M. Blow, J.J. Birktoft, and B.S. Hartley. Nature, **221**, 337 (1969); (*f*) D.M. Blow and T.A. Steitz. Annu. Rev. Biochem. **39**, 63 (1970); (*g*) D. Hadzi. J. Mol. Struct. **177**, 1 (1988); (*h*) R.L. Schowen. *In* Mechanistic principles of enzyme activity. *Edited by* J.F. Liebman and A. Greenberg. VCH Publishers, New York. 1988. p. 119; (*i*) K.B. Schowen and R.L. Schowen. Methods Enzymol. **87**, 551 (1982); (*j*) K.S. Venkatasubban and R.L. Schowen. CRC Crit. Rev. Biochem. **17**, 1 (1984); (*k*) P.F. Cook. Enzyme mechanisms from isotope effects. CRC Press, New York. 1992; (*l*) P.A. Frey, S.A. Whitt, and J.B. Tobin. Science, **264**, 1927 (1994); (*m*) J.A. Bibbs, M.P. Garoutte, B. Wang, P.D. Tittel, K.B. Schowen, and R.L. Schowen. Ber. Bunsen-Ges. Phys. Chem. **102**, 573 (1998).
6. A. Staib, D. Borgis, and J.T. Hynes. J. Chem. Phys. **102**, 2487 (1995), and references cited therein.
7. (*a*) P. Schuster, G. Zundel, and C. Sandorfy (*Editors*). The hydrogen bond. North Holland Publ. Co., Amsterdam. 1976; (*b*) J. Emsley, D.J. Jones, and J. Lucas. Rev. Inorg. Chem. **3**, 105 (1981); (*c*) B.S. Ault. Acc. Chem. Res. **15**, 103 (1982); (*d*) D. Mootz and K. Bartmann. Angew. Chem. **100**, 424 (1988); Angew. Chem. Int. Ed. Engl. **27**, 391 (1988); (*e*) H.J. Berthold, E. Preibsch, and E. Vonholdt. Angew. Chem. **100**, 1581 (1988); Angew. Chem. Int. Ed. Engl. **27**, 1527 (1988); (*f*) F. Hibbert and J. Emsley. Adv. Phys. Org. Chem. **26**, 255 (1990); (*g*) A. Novak. Struct. Bonding (Berlin), **18**, 177 (1974).
8. (*a*) G.S. Denisov, N.S. Golubev, V.A. Gindin, H.H. Limbach, S.S. Ligay, and S.N. Smirnov. J. Mol. Struct. **322**, 83 (1994); (*b*) N.S. Golubev, V.A. Gindin, S.S. Ligay, and S.N. Smirnov. Biochemistry (Moscow), **59**, 447 (1994); (*c*) N.S. Golubev, S.N. Smirnov, V.A. Gindin, G.S. Denisov, H. Benedict, and H.H. Limbach. J. Am. Chem. Soc. **116**, 12055 (1994); (*d*) S.N. Smirnov, N.S. Golubev, G.S. Denisov, H. Benedict, P. Schah-Mohammedi, and H.H. Limbach. J. Am. Chem. Soc. **118**, 4094 (1996); (*e*) N.S. Golubev, G.S. Denisov, S.N. Smirnov, D.N. Shchepkin, and H.H. Limbach. Z. Phys. Chem. **196**, 73 (1996); (*f*) N.S. Golubev, S.N. Smirnov, P. Schah-Mohammedi, I.G. Shenderovich, G.S. Denisov, V.A. Gindin, and H.H. Limbach. Russ. J. Gen. Chem. **67**, 1082 (1997); (*g*) I.G. Shenderovich, S.N. Smirnov, G.S. Denisov, V.A. Gindin, N.S. Golubev, A. Dunger, R. Reibke, S. Kirpekar, O.L. Malkina, and H.H. Limbach. Ber. Bunsen-Ges. Phys. Chem. **102**, 422 (1998); (*h*) N.S. Golubev, I.G. Shenderovich, S.N. Smirnov, G.S. Denisov, and H.H. Limbach. Chem. Eur. J. **5**, 492 (1999).
9. (*a*) G.S. Denisov and N.S. Golubev. J. Mol. Struct. **75**, 311 (1981); (*b*) N.S. Golubev, S.F. Bureiko, and G.S. Denisov. Adv. Mol. Relaxation Interact. Processes, **24**, 225 (1982); (*c*) N.S. Golubev, G.S. Denisov, and E.G. Pushkareva. J. Mol. Liq. **26**, 169 (1983); (*d*) N.S. Golubev and G.S. Denisov. J. Mol. Struct. **270**, 263 (1992).
10. (*a*) Th. Zeegers-Huyskens and P. Huyskens. Mol. Interact. **2**, 1 (1980); (*b*) G. Zundel and J. Fritsch. The Chemical Physics of Solvation, **2**, 21 (1986); (*c*) Z. Dega-Szafran and M. Szafran. Heterocycles, **37**, 627 (1994); (*d*) R. Lindemann and G. Zundel. J. Chem. Soc. Faraday Trans. 2, **68**, 979 (1972); (*e*) J. Chem. Soc. Faraday Trans. 2, **86**, 301 (1990); (*f*) Z. Dega-Szafran, A. Hrynio, and M. Szafran. J. Mol. Struct. **240**, 159 (1990); (*g*) G.V. Gusakova, G.S. Denisov, A.L. Smolyanski, and V.M. Schreiber. Dokl. Akad. Nauk SSSR, **193**, 1065 (1970); (*h*) Z. Dega-Szafran, M. Grunwald-Wyspianska, and M. Szafran. Spectrochim. Acta, Part A: **47A**, 125 (1991); (*i*) L. Sobczyk. J. Mol. Struct. **177**, 111 (1988); (*j*) Z. Dega-Szafran and E. Dulewicz. J. Chem. Soc. Perkin Trans. 2, 345 (1983); (*k*) Z. Dega-Szafran, M. Grunwald-Wyspianska, and M. Szafran. J. Chem. Soc. Faraday Trans. **87**, 3825 (1991); (*l*) S.E. Odinokov, A.A. Mashkovsky, V.P. Glazunov, A.V. Iogansen, and B.V. Rassadin. Spectrochim. Acta, **32A**, 1355 (1976); (*m*) V.P. Glazunov, A.A. Mashkovsky, and S.E. Odinokov. Spectrosc. Lett. **9**, 391 (1976); (*n*) S.E. Odinokov, A.A. Nabiullin, A.A. Mashkovsky, and V.P. Glazunov. Spectrochim. Acta, Part A: **39A**, 1055 (1983); (*o*) L.B. Jerzykiewicz, T. Lis, Z. Malarski, and E. Grech. J. Crystallogr. Spectrosc. Res. **23**, 805 (1993).
11. (*a*) H. Benedict, Ch. Hoelger, F. Aguilar-Parrilla, W.P. Fehlhammer, M. Wehlan, R. Janoschek, and H.H. Limbach. J. Mol. Struct. **378**, 11 (1996); (*b*) H. Benedict, H.H. Limbach, M. Wehlan, W.P. Fehlhammer, N.S. Golubev, and R. Janoschek. J. Am. Chem. Soc. **120**, 2939 (1998); (*c*) M. Ramos, I. Alkorta, J. Elguero, N.S. Golubev, G.S. Denisov, H. Benedict, and H.H. Limbach. J. Phys. Chem. A, **101**, 9791 (1997).
12. (*a*) M. Witanowski, L. Stefaniak, and G.A. Webb. Annu. Rep. NMR Spectrosc. **11** (1981); **(***b*) G. Martin, M.L. Martin, and J.P. Gouesnard. NMR, **18** (1989), and references cited therein.
13. (*a*) W. Saffioti and W.A. Bueno. J. Chim. Phys. Phys.-Chim. Biol. **73**, 731 (1976); (*b*) C.H. Rochester and S.A. Sclosa. J. Chem. Soc. Faraday Trans. 1, **75**, 2781 (1979); (*c*) Handbook of chemistry and physics. 62nd ed. CRC Press Inc., Boca Raton, Fla. 1981–1982. p. D.142; (*d*) K.L. Brown and E. Zahonyi-Budo. Inorg. Chem. **20**, 1264 (1981); (*e*) G. Kortüm, W. Vogel, and K. Angrussow. Dissociation constants of organic acids in aqueous solution. Butterworths, London. 1961; (*f*) In DMSO: F.G. Bordwell, X.M. Zhang, and J.P. Cheng. J. Org. Chem. **58**, 6419 (1993).
14. (*a*) L. Pauling. J. Am. Chem. Soc. **69**, 542 (1947); (*b*) I.D. Brown. Acta Crystallogr. Sect. B: Struct. Sci. **B48**, 553 (1992).
15. (*a*) P. Gilli, V. Bertolasi, V. Ferretti, and G. Gilli. J. Am. Chem. Soc. **116**, 909 (1994); (*b*) Th. Steiner and W. Saenger. Acta Crystallogr. Sect. B: Struct. Sci. **B50**, 348 (1994); (*c*) Th. Steiner. J. Chem. Soc. Chem. Commun. 1331 (1995); (*d*) J. Phys. Chem. A, **102**, 7041 (1998).
16. A.R. Ubbelohde and K.G. Gallagher. Acta Crystallogr. **8**, 71 (1955).